J. exp. Biol. 154, 439–461 (1990)
Printed in Great Britain

MEASURING AERODYNAMIC INTERFERENCE DRAG BETWEEN A BIRD BODY AND THE MOUNTING STRUT OF A DRAG BALANCE

BY VANCE A. TUCKER

Department of Zoology, Duke University, Durham, NC 27706, USA

Accepted 11 June 1990

Summary

1. The drag of a bird body mounted on the strut of a drag balance in a wind tunnel is more than the sum of the drags of the isolated strut and the isolated body. The strut changes the air flow around the body and generates additional drag, known as interference drag. This paper describes practical methods for measuring the drag of bird bodies: a strain-gauge drag balance, dimensions for struts made with machine or hand tools, and a procedure for correcting drag measurements for interference drag.

2. Interference drag can be measured by extrapolating a relationship between the drag of isolated struts with different cross-sectional sizes and shapes and the drag of a body mounted on those struts. The interference length – the length of an isolated strut that produces drag equal to the interference drag – is a useful quantity for predicting interference drag.

3. The relationship mentioned above is a straight line for a model peregrine falcon (*Falco peregrinus* L.) body mounted on smooth struts – struts with convex cross-sectional shapes ranging from streamlined to circular. This finding simplifies the determination of interference drag in three ways: (i) the line can be found from measurements with just two struts – a standard strut with low drag and a calibration strut with high drag; (ii) the two struts need not have the same shape – for example, the standard strut can be changed to a calibration strut by attaching a spoiler without disturbing the body mounted on the strut – and (iii) a single value of interference length (33.1 mm) describes smooth struts with a range of shapes and sizes. These struts had drag coefficients between 0.33 and 0.91 at Reynolds numbers between 2100 and 10 800.

4. The interference length of a strut supporting the actual falcon body with a feathered surface is not significantly different from that of the strut supporting the model body with a rigid surface.

5. As a hypothesis, interference length (h_I, in metres) of a smooth strut varies with the size of the body mounted on it:

$$h_I = 0.0365 m^{0.333},$$

where m is the body mass (in kg) of the intact bird.

Key words: drag coefficient, extrapolation method, interference length, model body, navy strut, peregrine falcon, *Falco peregrinus*.

6. 95 % of the interference drag appears to arise from a 15 mm length of the strut nearest the body.

Introduction

The aerodynamic drag on bird bodies is an important quantity in theoretical treatments of gliding and flapping flight (see review by Pennycuick, 1989). The usual method of measuring body drag involves mounting a frozen, wingless body on the strut of a drag balance in a wind tunnel (see Tucker, 1990). The drag of the body alone is taken to be the difference between the drag of the body on the strut and the drag of the strut alone.

However, this difference does not measure the drag of the isolated body, because the presence of the strut changes the air flow around the body and the strut and causes additional drag known as interference drag (Hoerner, 1965; Gorlin and Slezinger, 1966; Pankhurst and Holder, 1952; Pope and Harper, 1966). Interference drag may make up more than 20 % of the drag measured by the drag balance (Tucker, 1990).

Tucker (1990) described an extrapolation method suitable for measuring interference drag on bird bodies. The method establishes an empirical mathematical relationship between the drag of the body on a strut and the drag of the strut alone for different types of struts. It then extrapolates the relationship to find the drag of a body mounted on a strut with no drag, i.e. the drag of the isolated body. The interference drag is the drag of the body mounted on the strut minus the drag of the isolated strut minus the drag of the isolated body.

This study investigates how the relationship mentioned in the previous paragraph depends on the types of strut used to establish the relationship. The results show that the relationship is independent of strut size and shape for certain types of struts, that the relationship can be established with just two struts, and that the interference drag generated by a strut can be predicted from the drag of the isolated strut. The study demonstrates a practical method for measuring interference drag and confirms the value of the body drag coefficient found for a peregrine falcon (*Falco peregrinus*) in an earlier study (Tucker, 1990).

Strut definitions

Two characteristics define a strut: length and cross-section. The length is the distance between the point where the strut exits from the shroud of the drag balance and the point where it contacts the body mounted on it. The cross-section (Fig. 1A) is the perimeter of the strut in a plane perpendicular to the length and is the same at all points along the length. The cross-section is symmetrical about an axis of symmetry parallel to the direction of air flow. The leading point is the intersection between the axis of symmetry and the blunter, upwind end of the cross-section. The trailing point is a similar point at the sharper, downwind end of the cross-section.

The chord is the distance from the leading to the trailing point. The thickness is

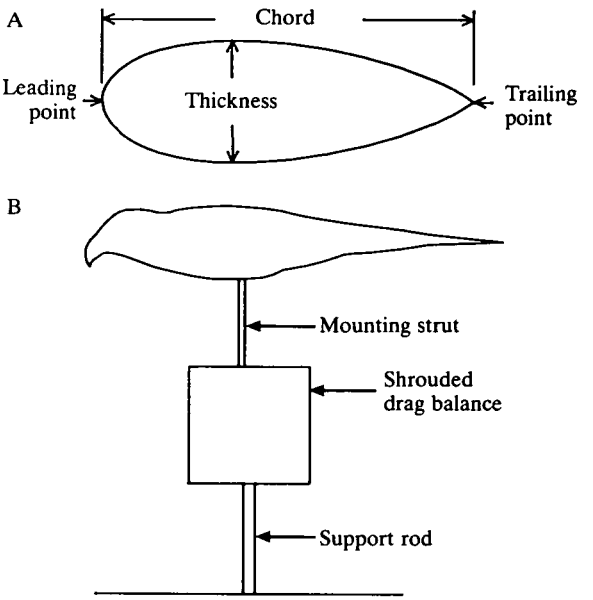

Fig. 1. (A) Cross-section of a strut, showing chord, thickness and leading and trailing points. (B) Falcon body on a strut attached to a drag balance covered with a shroud. The body is 0.447 m long, measured from the tip of the tail to the front of the beak, with the head, torso and tail positioned for minimum drag.

the maximum width of the cross-section along an axis perpendicular to the axis of symmetry. The fineness is the chord divided by the thickness.

Cross-sections may have different shapes, defined by an equation or a table of dimensionless, standard x,y coordinates for a half of a standard cross-section. The coordinate system originates at the leading point of the standard cross-section, and x increases along the axis of symmetry to a value of 1 at the trailing point. y increases along a perpendicular axis to a value of 1 at the maximum width of the cross-section. The x and y coordinates of an actual cross-section equal the desired chord multiplied by the standard x coordinates, and half the desired thickness multiplied by the standard y coordinates, respectively.

Each standard cross-section defines a strut type. One type of strut may have a variety of sizes and shapes depending on its chord and thickness. For example, this study uses three struts of a circular type with different diameters, three struts of a streamlined type with different chords and thicknesses, and one strut of another streamlined type.

Theory

Types of drag

The measured drag (D_m) on a body mounted on the strut of a drag balance may be subdivided into three terms:

$$D_m = D_B + D_s + D_I, \quad (1)$$

where D_B is the drag of the isolated body, D_s is the drag of the strut with nothing mounted on it and D_I is the interference drag generated by both the strut and the drag balance. The interference drag from the drag balance is negligible in this study because of the length of the strut. Tucker (1990) describes a method for determining how long the strut must be to eliminate interference drag from the drag balance.

Strut drag

Strut drag depends on dynamic pressure (q), the strut length (h, for height), the strut thickness (t) and the drag coefficient of the strut (C_D):

$$D_s = qhtC_D . \tag{2}$$

The dynamic pressure is constant in this study, and is given by:

$$q = 0.5\rho V^2 , \tag{3}$$

where ρ is the density of air and V is the speed of the air flowing past the strut. These relationships, and others in this section, are conventions that can be found in books on aerodynamics (e.g. von Mises, 1959) or in books that describe aerodynamics in a biological context (e.g. Pennycuick, 1989; Vogel, 1981).

I changed the drag of struts by varying the chord while holding the fineness constant. The chord of the strut can be introduced into equation 2 by replacing t with the ratio of chord (c) to fineness (f):

$$D_s = qhcC_D/f . \tag{4}$$

The drag coefficient depends on Reynolds number (Re), which itself depends on chord:

$$Re = \rho cV/\mu , \tag{5}$$

where μ is the viscosity of air (constant in this study). The ratio ρ/μ (the reciprocal of kinematic viscosity) has the value $68\,436\,\mathrm{s\,m^{-2}}$ for air at sea level in the US standard atmosphere (von Mises, 1959). C_D is found at different Re values by measuring the quantities on the right-hand side of equation 6:

$$C_D = D_s/(qht) , \tag{6}$$

which is simply a rearrangement of equation 2.

I assume that strut drag is proportional to length (h) when all the other variables in equation 4 are constant:

$$D_s = rh , \tag{7}$$

where r is a constant strut drag per unit length.

This assumption is probably not strictly correct. The drag per unit length of circular cylinders oriented with the cylinder axis perpendicular to the direction of air flow increases with length because of flow around the ends of the cylinders (Goldstein, 1965). However, the assumption will serve for present purposes since struts for bird bodies have a limited range of lengths and have one end shielded by the drag balance.

Interference drag

Conventional methods for measuring interference drag on aircraft use combinations of multiple mounting struts (Gorlin and Slezinger, 1966; Pope and Harper, 1966). The extrapolation method for bird bodies is novel (Tucker, 1990), and this section uses new terminology and derivations to describe it.

The interference length (h_I) is the length of strut that has the same strut drag as the interference drag D_I:

$$h_I = D_I/r . \tag{8}$$

Equation 1 can be expressed in terms of h_I by combining equations 7 and 8,

$$D_I = D_s h_I/h \tag{9}$$

and substituting equation 9 into equation 1:

$$D_m = D_s(1 + h_I/h) + D_B . \tag{10}$$

I assume that D_I is independent of strut length for practical struts, since the interference drag appears to arise from the 15 mm length of the strut nearest the body (see Discussion). Hence, h_I is independent of strut length, but it may change with D_s.

Equation 10 provides the rationale for the extrapolation method of measuring interference drag. If a curve relating D_m to D_s is found by making measurements on a body mounted on different struts of constant length, the curve can be extrapolated to D_s=0, where D_m=D_B. Once body drag is known, the interference drag ($D_{I,0}$) for a strut with drag $D_{s,0}$ and measured drag $D_{m,0}$ can be calculated with equation 1:

$$D_{I,0} = D_{m,0} - D_{s,0} - D_B . \tag{11}$$

The curve must be found empirically because h_I depends on D_s in an unknown way, and it must be extrapolated because an actual strut cannot have zero drag and still be strong enough to support the body.

Fig. 2 illustrates the method for a linear curve relating D_m to D_s. The curve has a constant slope, which indicates that the interference length does not vary with D_s. This can be seen from the derivative (the slope) of equation 10 for a constant h_I:

$$dD_m/dD_s = 1 + h_I/h . \tag{12}$$

Rearranging equation 12,

$$h_I = h[(dD_m/dD_s) - 1] . \tag{13}$$

In fact, h_I is constant for several struts of different types and chords investigated in this study, which greatly simplifies the measurement of interference drag.

Effect of body size and shape, and speed, on strut drag and interference drag

Investigators may find the extrapolation method useful for a variety of bodies arranged in different configurations and exposed to different air speeds. This paper does not attempt to predict h_I and C_D under all conditions.

Instead, the measurement methods described herein should be used. A

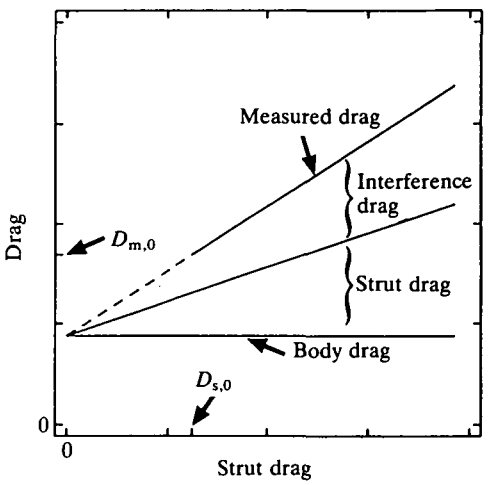

Fig. 2. Theoretical relationships between body, strut, interference and measured drag. The dashed line is an extrapolation beyond the point for the drag ($D_{s,0}$) of the smallest strut alone and the measured drag ($D_{m,0}$) of a body mounted on that strut.

plausible first assumption is that neither h_l nor C_D change appreciably with speed. It follows that C_D and h_l can be determined at a particular speed and used with equations 2 and 9 to calculate D_s and D_l at other speeds.

Materials and methods

Wind tunnel

I measured drag on the frozen body of a peregrine falcon (*Falco peregrinus* L.) and a model body mounted on a drag balance (Fig. 1B) in an open-circuit wind tunnel set to an equivalent air speed of $12.6\,m\,s^{-1}$. (The actual air speed produced the same dynamic pressure (q) as an air speed of $12.6\,m\,s^{-1}$ in the US standard atmosphere at sea level (von Mises, 1959).) The wind tunnel had a rectangular working section with a cross-sectional area of $1.5\,m^2$. Tucker and Parrott (1970) and Tucker and Heine (1990) give a more complete description of the tunnel and its calibration.

Frozen and model bodies

The frozen body was wingless, and its head, torso and tail were positioned for minimum drag. The model body was made of rigid plastic foam and was hollow. The shape of its smooth surface accurately duplicated the feathered surface of the frozen body. I used these same bodies in a previous study (Tucker, 1990), which describes them in more detail.

The mounting struts from the drag balance attached to the frozen body and the model at a point in the mid-ventral line, half-way from the anterior end of the sternum to the posterior end. Each strut ended in a threaded rod, 3.18 mm in

diameter, that either screwed into a wooden insert frozen into the frozen body or passed through a hole in the model. A nut could be placed on the threaded rod inside the model through a larger hole in the mid-dorsal line. I covered this hole with tape when measuring drag. I rotated the frozen body and the model around the threaded rod to align their long axes with the direction of air flow.

Drag balance

The drag balance had three parts: a force transducer, mounts and a streamlined shroud (Fig. 3). The force transducer was of the parallelogram type described by Gorlin and Slezinger (1966). I milled it out of aluminium plate 6.35 mm thick, with arms 1.14 mm thick. Four strain gauges glued to the arms with cyanoacrylate cement formed a Wheatstone bridge.

A 5 V power supply excited the bridge, and an amplifier multiplied the voltage from the bridge by 100 to produce approximately 0.12 mV mN^{-1} of drag. A digital voltmeter (Acculex model 950) displayed the voltage from the amplifier. The voltmeter reduced electrical noise by (1) using a dual-slope analogue-to-digital converter that integrated the analogue voltage over a 0.2 s conversion period, and (2) using a microprocessor that averaged eight successive digital conversions. The bridge was at least 1000 times more sensitive to drag than to a vertical force applied at right angles to the drag direction.

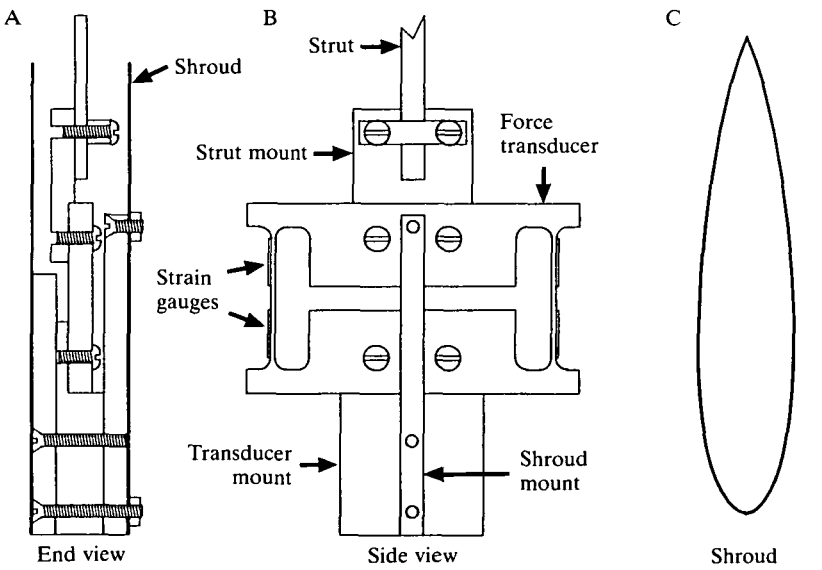

Fig. 3. End (A) and side (B) views of the drag balance, and a top view (C) of the streamlined shroud. The end view is a cross-section that shows the shroud in place. The side view is drawn with the shroud removed and shows the thin, vertical arms of the force transducer and the strain gauges cemented to them. The strut (drawn cut off) carries the bird body, and drag on the strut and body deforms the vertical arms. The drawings have the same scale, and the shroud has a chord of 130 mm measured from leading point to trailing point.

Aluminium mounts supported the force transducer, the strut and the streamlined shroud. A tapped hole in the transducer mount received the cut-down, threaded end of a steel rod 12.70 mm in diameter that extended through a hole in the floor of the wind tunnel from a tripod on the laboratory floor. The rod isolated the drag balance from the wind tunnel, and I tilted it to align the force transducer with the direction of air flow in the tunnel.

The strut mount clamped onto the end of the strut. I tilted the strut back and forth in the mount to align reference points on the beak and tail of the frozen body and the model to within 1 mm of fixed heights above the tunnel floor. This adjustment minimized drag and ensured that the frozen body and the model had the same angle of attack in all experiments.

The streamlined shroud shielded the transducer and the mounts from the wind. I made the shroud by shaping an aluminium sheet 0.51 mm thick to the cross-section of a Navy Number 1 strut type (see Table 1) with a thickness of 26.0 mm and a chord of 130.0 mm. Two nuts held the shroud firmly to one of the shroud mounts, and tape held the trailing edges of the shroud together. This arrangement allowed the shroud to be lowered for access to the strut mount.

I calibrated the drag balance with weights hanging from the end of a thread that ran over a pulley with a low-starting-torque ball bearing (New Hampshire Bearing SR168). The other end of the thread attached to the tail of the frozen or model body, or to the top of the strut in experiments with isolated struts. The pulley changed the force transmitted from the weight to the drag balance by less than 1 mN (the bias of the drag balance). The voltage from the Wheatstone bridge was linearly related to weight within the imprecision of the drag balance. Imprecision, expressed as the standard deviation of repeated measurements of the same force, was less than 0.1 mN for the weights and less than 1.5 mN for the struts and bodies with the wind tunnel turned on.

Strut types

I used several different types of struts, all of which extended 93 mm from the top of the shroud to the frozen or model bodies. This length eliminated interference drag between the shroud and the body, since measurements showed that a strut length of 80 mm minimized the measured drag of the model (see Tucker, 1990, for an explanation of shroud interference). The 80 mm strut length is three times the thickness of the shroud cross-section, the same factor that minimized drag measured by another drag balance with a differently shaped shroud (Tucker, 1990).

Navy Number 1 struts

Three struts of this type (Fig. 4A and Table 1), henceforth referred to as navy struts, all had a nominal fineness of 2.94, but chords of 6.35 mm, 12.70 mm and 36.58 mm. Navy struts with a fineness close to 3 had lower drag coefficients than any other known strut type at the time they were designed (Beisel and Diehl, 1923; Diehl, 1928). I machined the struts from aluminium, or steel in the case of the

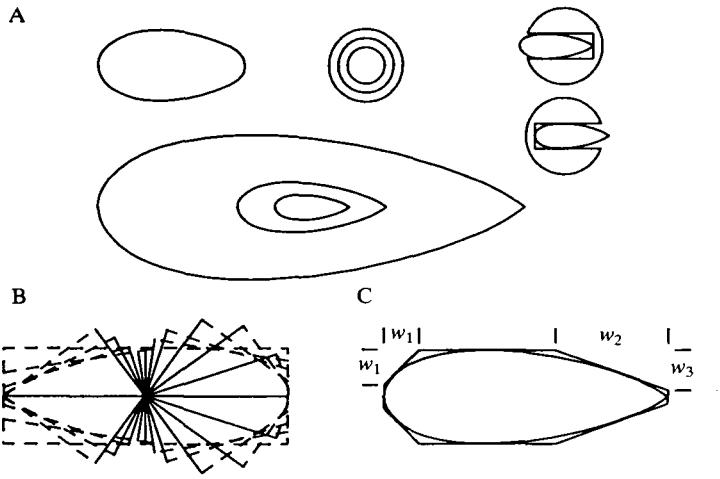

Fig. 4. (A) Cross-sections of all the struts used in this study, drawn to the same scale. The nested, streamlined cross-sections at the centre illustrate the navy struts, the largest of which had a chord of 36.6 mm. The nested cross-sections at the top centre illustrate the circular struts. The cross-section of the commercial strut is at the top left. The spoiled strut cross-sections at the top right show the spoiler on both the leading and trailing edges of the smallest navy strut. The simplified navy strut cross-section was similar to that of the intermediate-sized navy strut. (B) Cross-section of a strut cut from a solid piece of metal by a milling machine and an indexing head. Dashed lines show the milled flat surfaces. Solid lines (radii) are perpendicular to the dashed lines. Table 2 gives the lengths and angles of the radii for a Navy Number 1 strut with fineness 2.94. Filing the corners smooth between the flats finishes the strut. (C) Cross-section of a simplified navy strut (smooth curve) cut from a solid piece of metal with a rectangular cross-section and a chord three times longer than its thickness (t). The four corners of the piece of metal have been milled or filed flat to produce eight corners with the following dimensions: $w_1=0.375t$, $w_2=1.180t$, $w_3=0.429t$. The flats have angles of 45 and 20° to the axis of symmetry. Filing the eight corners to the smooth curve finishes the strut.

smallest one. The machining process began with a workpiece, typically a rod, mounted horizontally on the table of a vertical milling machine between an indexing head and a tail stock. The indexing head rotated the rod around its long axis in 20 angular steps. At each angle, I milled a flat surface along the length of the rod at a precise distance from its long axis (Fig. 4B and Table 2). The flat surfaces approximated the cross-section of the strut, and I filed down the corners between them to finish the strut. The actual fineness values of the struts varied from 2.58 for the smallest to 2.94 for the largest, because the smaller struts bowed away from the cutting tool during the milling process.

The end of the strut that fitted into the mount on the force transducer had flat sides, parallel to its plane of symmetry. I drilled and tapped the other end to receive the threaded rod that fitted into the frozen body or the model. The tapped end of the smallest strut was left rod-shaped to support the tapped hole. The rod-

Table 1. *Standard coordinates for Navy Number 1 strut type**

x	y	x	y
0.000	0.000	0.350	1.000
0.013	0.260	0.400	0.995
0.025	0.371	0.500	0.950
0.050	0.525	0.600	0.861
0.075	0.636	0.700	0.732
0.100	0.720	0.800	0.562
0.125	0.785	0.900	0.338
0.150	0.836	0.950	0.190
0.200	0.911	0.980	0.078
0.250	0.959	1.000	0.000
0.300	0.988		

* From von Mises (1959) or Diehl (1928).

Table 2. *Angles and radii for navy strut of fineness 2.94*

Angles*	Radius†	Angles	Radius
0, 360	0.500	90, 270	0.170
18, 342	0.483	99, 261	0.161
36, 324	0.424	108, 252	0.184
54, 306	0.337	117, 243	0.234
72, 288	0.246	126, 234	0.294
81, 279	0.203	180, 180	0.500

* Measured from axis of symmetry.
† Expressed as a fraction of chord.

shaped portion fitted into a recess in the frozen body and the model, and was not exposed to the air flow.

Simplified navy strut

This strut type can be made by a milling machine equipped with a vice instead of an indexing head, or by hand-filing. I investigated it to provide information on a strut that is easier to make than a standard navy strut, yet still is suitable for use with a drag balance.

A rectangular workpiece with four flats cut on it approximated the cross-section of a navy strut of fineness 3 (Fig. 4C). The flats served as guides for hand-filing the strut to its final form. I set the head of the milling machine to just two angles – 20 and 45° – and cut all four flats by rotating the workpiece end-for-end in the vice. Alternatively, I could have filed the flats by hand between lines scribed on the four sides of the work piece. The simplified navy strut used in this study had a fineness of 2.95 and a chord of 12.0 mm.

Commercial strut

I made this strut from streamlined aluminium tubing bought at a store that sold supplies for model aeroplanes. The cross-section of the tubing had a chord of 12.6 mm, a fineness of 2.05 and was thicker near the trailing point than a navy strut with the same chord (Fig. 4A).

Circular struts

These struts were steel or aluminium rods with circular cross-sections and diameters of 3.18, 4.76 and 6.35 mm (Fig. 4A). The diameter of a circular strut equals its thickness and chord.

I made a special circular strut for investigating the effect of a gap between the strut and the model on interference drag. This strut was a threaded rod, 3.18 mm in diameter covered by a sleeve 6.35 mm in diameter. The rod supported the model, and the sleeve could be moved up and down the rod to adjust the size of the gap between the sleeve and the model.

Spoiled struts

A spoiled strut is a streamlined strut with a spoiler attached that increases the drag of the strut. The spoiler in this study was a grooved wooden rod that fitted over the entire leading or trailing edge of the smallest navy strut (Fig. 4A). I made the spoiler by milling a groove along the length of a wooden dowel 6.60 mm in diameter.

Experimental protocol

The measured drag values reported in the text or graphs for a body on a strut are means of 3–5 sequential measurements. The sequence began with a reading from the drag balance with the wind tunnel turned off, then with the tunnel turned on, and so forth for each measurement in the series. The paired readings compensated for any drift in the drag balance output. After three sequences, I calibrated the drag balance by reading it with the thread from the calibrating weight attached to the body or the strut and again with the thread detached.

I used the same sequential process to measure the drag of isolated struts. Strut drag values are grand means – means of 2–3 means of sequential measurements.

Results

Relationship between strut drag and measured drag of the model body

The relationship between strut drag and measured drag was linear for all but the spoiled struts (Fig. 5):

$$D_m = 1.356D_s + 83.2 \quad (14)$$

(drag in mN, standard deviation around line=1.42, N=21).

The spoiled struts produced measured drag values that fell above the line in Fig. 5. The spoiled strut with the spoiler pressed over the trailing edge had less

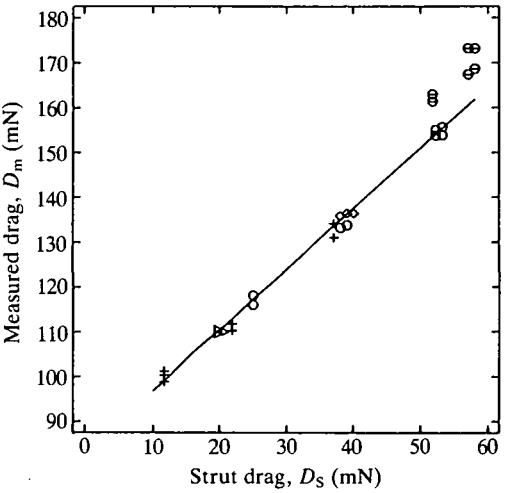

Fig. 5. Strut drag and measured drag values for the model body mounted on various struts: navy struts (crosses), simplified navy strut (triangles), commercial strut (squares), circular struts (circles) and spoiled struts (split circles). The spoiled strut has greater drag with the spoiler on the leading edge than on the trailing edge. Some overlapping points are shifted horizontally to separate them slightly.

drag than with the spoiler pressed over the leading edge. Combining the data for both spoiled struts yields a mean spoiled strut drag of 54.4 mN and a mean measured drag of the model on the spoiled struts of 166.4 mN.

Drag coefficients of struts

The streamlined struts had lower drag coefficients than the circular ones (Fig. 6). The smaller navy struts, including the simplified type, had C_D values that were about 60% of those of circular struts with the same thickness. The commercial strut was less effective at reducing drag. Its C_D was 74% of that of a circular strut of the same thickness.

Drag coefficients of both streamlined and circular struts are known to change with Reynolds number (Goldstein, 1965). Only the navy struts varied enough in size to show a marked dependence of C_D on Reynolds number. Some of the decrease in C_D for the largest navy strut may be due to its greater fineness.

Effect of a gap between the strut and the model body

Measured drag increased as the gap between the strut and the model increased from 0 to 6.4 mm (Fig. 7).

Drag of the frozen body

The mean measured drag of the frozen body on the spoiled strut (spoiler on leading edge) was 239.6 mN (N=2), and on the smallest navy strut was 171.2 mN (N=2). The mean strut drags of the spoiled and navy struts were 57.1 and 11.7 mN, respectively.

Discussion

The struts used in this study fall into two categories, depending on the relationship between the drag of the strut and the measured drag of the model body mounted on it. Graphically, this relationship is a straight line for smooth struts. I shall call this line the smooth strut line. Smooth struts have a fineness of 1

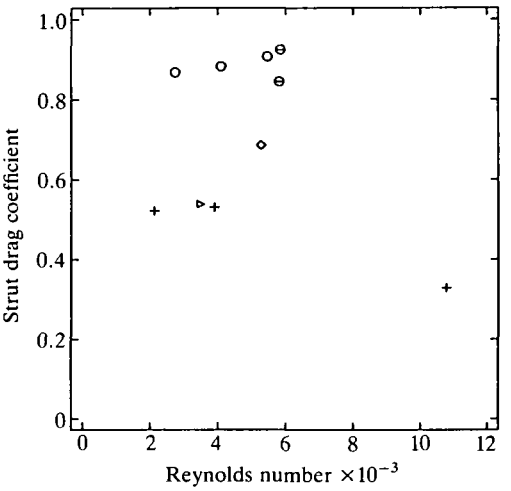

Fig. 6. Mean drag coefficients of various struts at different Reynolds numbers: navy struts (crosses), simplified navy strut (triangle), commercial strut (square), circular struts (circles) and spoiled struts (split circles). The spoiled strut has a higher drag coefficient with the spoiler on the leading edge than on the trailing edge.

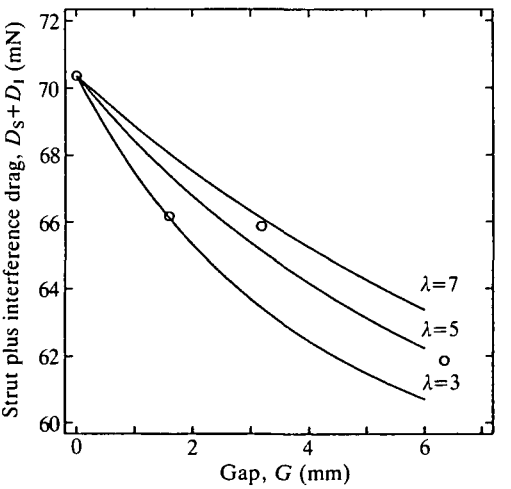

Fig. 7. The effect of gap width on drag. The horizontal axis shows the width of the gap between the sleeve of the special circular strut and the model body. The vertical axis shows the difference between measured drag and body drag (the sum of strut drag and interference drag). Circles are measured values, and curves are theoretical predictions for three different space constants (λ, see Appendix).

or more and cross-sections that are everywhere outwardly convex. They comprise the navy, simplified navy, commercial and circular struts.

Data for spoiled struts fall above the smooth strut line. Spoiled struts have cross-sections with discontinuities. They comprise the smallest navy strut with the spoiler pressed on either the leading or trailing edge.

The smooth strut line

The existence of this line greatly simplifies the determination of interference drag for the following reasons.

(1) The equation of the line can be derived from measurements on just two struts (see Appendix for sample calculations). One of these struts (the standard strut) can be the strut ordinarily used with the drag balance. It should have low drag, i.e. it should be streamlined and as small as practical. The other (the calibration strut) must have greater drag.

(2) Smooth struts need not have precisely defined cross-sections. Apparently any smooth cross-section will do, since struts with cross-sections ranging from streamlined to circular qualify as smooth struts. For example, the standard strut could be filed to shape by hand, and the calibration strut could be cut from a rod of circular cross-section. The cross-section should be symmetrical and constant along the strut length.

The most convenient calibration strut is one made by attaching a spoiler to the standard strut. In this case, the standard strut becomes the calibration strut without disturbing the bird body on the drag balance. Although a spoiled calibration strut is not smooth, the error in estimating body drag can be made small and corrected for. I shall discuss this error in a later section.

(3) A single interference length of 33.1 mm describes all the smooth struts in this study, regardless of their type or chord, and hence drag coefficient. This value comes from substituting the slope of the smooth strut line into equation 13. The interference length also is independent of strut length and air speed, according to plausible assumptions (see Theory).

Interference length and other bird bodies

The single interference length for smooth struts suggests that the interference drag for all bodies mounted on smooth struts of any chord and length could be calculated from an interference length of 33.1 mm (see Appendix for sample calculations). Such calculations may be accurate for bird bodies that are similar in size and shape to the model in this study and attach to the strut in the mid-ventral line. However, the interference length may depend on body size and shape, attachment point of the strut or struts, and orientation of the body to the air flow. Whether the surface of the body is feathered or rigid did not significantly affect the interference length in this study, as will be discussed in a later section.

The interference length probably depends on the dimensions of the body mounted on the strut. For example, Hoerner (1965, pp. 8–10) notes that interference drag arises from the region of the strut nearest to the body. He

suggests that the length of this region is 16% of the body diameter. As a hypothesis, the interference length of a smooth strut attached to the ventral midline of a bird body could be taken as proportional to the effective diameter of the body (d_B), where d_B is the diameter of a circle that has the same area as the maximum cross-sectional area of the body (S_B) along the longitudinal axis. Thus:

$$d_B = 2(S_B/\pi)^{1/2}. \quad (15)$$

The model body had an S_B value of 0.00669 m^2 (Tucker, 1990) and a d_B value of 92.3 mm. The interference length was 35.9% of the d_B value.

This percentage can be used to estimate the interference length of smooth struts for birds of different sizes because S_B is a function of the body mass (m) of the intact bird (Pennycuick *et al.* 1988):

$$S_B = 0.00813m^{0.666}. \quad (16)$$

Combining equations 15 and 16 with the percentage for the model yields a relationship between interference length (in metres) and body mass (in kg):

$$h_I = 0.0365m^{0.333}. \quad (17)$$

Equation 17 should be viewed primarily as a hypothesis to be tested. Even so, it should give better estimates of interference drag than the usual practice of neglecting interference drag altogether (Tucker, 1990).

Spoiled struts as calibration struts

A spoiled strut is particularly suitable as a calibration strut for frozen bodies, which steadily thaw. A spoiler may be attached to the standard strut quickly without ruffling the feathers or changing the position of body parts. However, the spoiled struts in this study generated more interference drag than the smooth struts. The extra interference drag causes an error in estimating body drag by the extrapolation method. This section shows how the error can be kept small and corrected for.

The measured drag of the model body mounted on a spoiled strut fell at a point above the smooth strut line. The extra interference drag is the distance between this point and the line. The spoiled strut line is the line between this point and the point on the smooth strut line for the standard strut drag (see Fig. 9). The spoiled strut line extrapolates to an erroneous body drag, which is less than that found by extrapolating the smooth strut line.

The error, however, is only a fraction of the extra interference drag. The fraction is the drag of the standard strut divided by the drag added to the strut by the spoiler, and it can be kept small by using a standard strut with low drag.

For example, the drag of the smallest navy strut was 0.21 of the mean drag added by the spoiler. (Mean drags in this section are means for the spoiler added to the leading edge and the trailing edge of the standard strut.) The mean measured drag of the model on the spoiled strut was 9.4 mN above the smooth strut line. Thus, the body drag determined by extrapolating the spoiled strut line is

$0.21 \times 9.4 = 2.0$ mN less than the correct body drag determined by extrapolating the smooth strut line – a 2.4 % error.

This error can be eliminated by using the extra interference length to calculate the position of the smooth strut line. The extra interference length is analogous to the interference length: it is the length of a spoiled strut that has the same strut drag as the extra interference drag. Continuing the analogy, I assume that a single extra interference length describes spoiled struts with different chords and lengths at different air speeds.

The extra interference length is the extra interference drag divided by the drag per unit length (r in equation 7) of the spoiled strut. It has a value of 16.1 mm (see Appendix) for the model body on the spoiled strut. An example in the Appendix shows how to use the extra interference length to find the smooth strut line for the frozen body.

The effect of feathers on body and interference drag

I measured the drag of the frozen body mounted on the smallest navy strut as the standard strut, and on a calibration strut made by pressing the spoiler over the leading edge of the standard strut. The equation of the smooth strut line calculated from these data and the extra interference length was:

$$D_m = 1.289 D_s + 156.1 \tag{18}$$

(see Appendix for derivation).

The intercept of equation 18 yields a value for body drag that can be compared with another measurement on the same body made with a different drag balance and struts (Tucker, 1990). The drag coefficient of the body ($C_{D,B}$) in the present study, given by:

$$C_{D,B} = D_B/(qS_B), \tag{19}$$

is 0.24, where S_B is the maximum cross-sectional area of the body (0.00669 m^2, Tucker, 1990). This drag coefficient is slightly higher than the value of 0.23 reported in Tucker (1990). The discrepancy is in the expected direction, since the earlier study did not correct for the extra interference drag of the spoiled strut. The drag coefficient of the model, however, is slightly lower than that in the earlier study (0.13 *vs* 0.14), a discrepancy opposite to that expected.

Tucker (1990) reported that the drag coefficient of the model body was only 59 % of that for the frozen body at an air speed of 12.4 $m\,s^{-1}$, and attributed the difference to the drag of the feathers. In the present study, the drag coefficient of the model was 54 % of that for the frozen body.

Does the feathered surface of the frozen body rather than the rigid surface of the model influence interference length? The smallest navy strut supporting the frozen body had a smaller interference length (26.1 mm, from equations 13 and 18) than that (33.1 mm) for smooth struts supporting the rigid model. This difference is not significant, since the standard deviation of h_I for the frozen body is 6 mm. This value comes from a propagation of error analysis (Ku, 1969, p. 331) of the imprecisions of the measured values used to calculate h_I.

Effect of a gap between the strut and the model body

These experiments show how the closeness of fit between the strut and the body affects interference drag. I adjusted the gap between the strut and the body by moving the sleeve of the special circular strut up and down the rod that supported the body. As the gap widened, the measured drag gradually decreased (Fig. 7).

A mathematical model (see Appendix) accounts for the effect of the gap by treating measured drag as the sum of several terms: the body drag, the interference drag from both the rod and the sleeve, and the non-interference drag from both the rod and the sleeve. The interference drag decreases as the gap widens because the interference drag of the rod exposed in the gap is less than that of the larger sleeve. Likewise, the non-interference drag decreases because the drag of the rod is less than that of the sleeve.

The model treats the interference drag of the rod and the sleeve as exponential functions of gap width. These functions fit the measured data reasonably well when 95 % of the interference drag arises from a region of the strut 15 mm long nearest the body (a space constant λ of 5 mm in Fig. 7). This length seems plausible; Hoerner (1965) also suggests a length of 15 mm (see Appendix). It should not be taken too seriously, because it depends on small changes in drag and on the exponential model for interference drag. Other models that fit the observations may give different lengths.

Appendix

The slope (dD_m/dD_s) and intercept (D_B) of the smooth strut line

Example 1 shows how to use measurements from a smooth standard strut and a smooth calibration strut. Example 2 shows how to use measurements from a smooth standard strut and a calibration strut made by attaching a spoiler to the standard strut. Fig. 8 shows the smooth strut line and the variables described below.

$D_{s,std}$=drag of the standard strut.

$D_{s,cal}$=drag of the calibration strut.

$D_{m,cal,sm}$=measured drag of a body on a smooth calibration strut.

$D_{m,cal,sp}$=measured drag of a body on a spoiled calibration strut.

In both examples, the slope is:

$$dD_m/dD_s = (D_{m,cal,sm} - D_{m,std})/(D_{s,cal} - D_{s,std}), \quad (20)$$

and the intercept is:

$$D_B = D_{m,std} - dD_m/dD_s \times D_{s,std}. \quad (21)$$

Example 1

Measure $D_{m,std}$, $D_{s,std}$, $D_{m,cal,sm}$ and $D_{s,cal}$. Calculate the slope and intercept with equations 20 and 21.

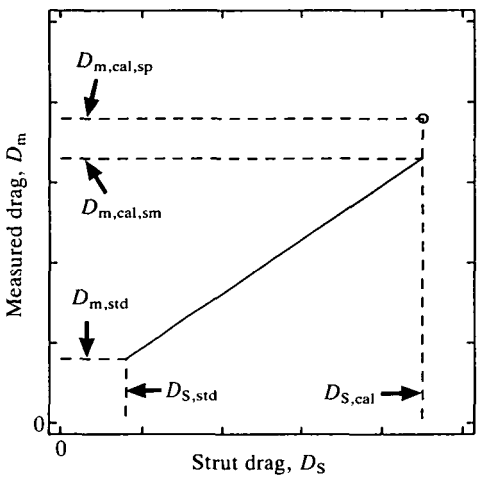

Fig. 8. Diagrammatic relationship between the smooth strut line and the measured drag of the model mounted on a spoiled strut. See Discussion for an explanation of the line and Appendix for an explanation of the symbols.

Example 2

Measure $D_{m,std}$, $D_{s,std}$, $D_{m,cal,sp}$, $D_{s,cal}$ and strut length (h). Given the extra interference length ($h_{I,ex}$), calculate:

$$D_{m,cal,sm} = D_{m,cal,sp} - h_{I,ex}D_{s,cal}/h\,, \tag{22}$$

and then calculate the slope and intercept with equations 20 and 21.

Interference length (h_I), interference drag (D_I) and extra drag (D_{ex})

The extra drag (D_{ex}) is the sum of the interference drag and the strut drag, and subtracting it from measured drag yields body drag. Example 1 shows how to estimate D_I and D_{ex} without measuring strut drag. Example 2 shows how to estimate both quantities if strut drag is measured.

Example 1

Measure D_m, h and t. Given: h_I, C_D for the strut. From equation 2:

$$D_I = qh_I tC_D \tag{23}$$

and

$$D_{ex} = q(h + h_I)tC_D\,. \tag{24}$$

Example 2

Measure D_m, D_s and h. Given: h_I. Calculate D_I with equation 9 and, from equation 10:

$$D_{ex} = D_s(1 + h_I/h)\,. \tag{25}$$

Extra interference length ($h_{I,ex}$)

Fig. 9 shows the variables described below.

Measurements

$D_{s,cal}$=mean drag of the smallest navy strut with the spoiler on its leading edge, and on its trailing edge
=54.4 mN.

$D_{m,cal,sp}$=mean measured drag of the model mounted on the smallest navy strut with the spoiler on its leading edge, and on its trailing edge
=166.4 mN.

Calculations

$D_{m,cal,sm}$=157.0 mN (calculated by substituting $D_{s,cal}$ into equation 14 for the smooth strut line).

The extra interference drag ($D_{I,ex}$) is 9.4 mN, given by:

$$D_{I,ex} = D_{m,cal,sp} - D_{m,cal,sm} . \quad (26)$$

The drag/length (r) for the calibration strut (h=93 mm) is 0.585 mN mm^{-1}, given by:

$$r = D_{s,cal}/h .$$

The extra interference length ($h_{I,ex}$) is 16.1 mm, given by:

$$h_{I,ex} = D_{I,ex}/r . \quad (27)$$

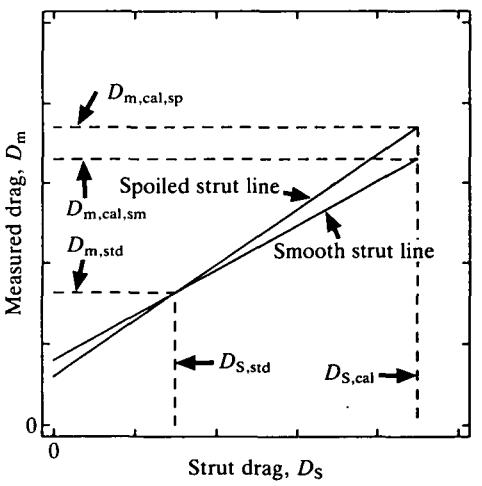

Fig. 9. Diagrammatic relationship between the smooth strut line and the spoiled strut line. See Discussion for an explanation of the lines and Appendix for an explanation of the symbols.

The smooth strut line for the frozen body

Given $h_{I,ex}$=16.1 mm. Fig. 9 shows the variables described below.

Measurements

$D_{s,std}$=drag of the smallest navy strut
=11.7 mN.

$D_{s,cal}$=drag of the smallest navy strut with the spoiler on the leading edge
=57.1 mN.

$D_{m,std}$=measured drag of the frozen body on the standard strut
=171.2 mN.

$D_{m,cal,sp}$=measured drag of the frozen body on the spoiled standard strut
=239.6 mN.

Calculations

Drag/length (r) for the calibration strut (h=93 mm) is 0.614 mN mm^{-1}, given by:

$$r = D_{s,cal}/h\,.$$

The extra interference drag ($D_{I,ex}$) is 9.9 mN, given by:

$$D_{I,ex} = rh_{I,ex}\,.$$

The calculated drag of the frozen body on the smooth calibration strut ($D_{m,cal,sm}$) is 229.7 mN, given by:

$$D_{m,cal,sm} = D_{m,cal,sp} - D_{I,ex}\,. \tag{28}$$

Equation of the smooth strut line

From equations 20 and 21,

$$dD_m/dD_s = 1.289$$

and

$$D_B = 156.1\text{ mN}\,.$$

Effect of a gap between the strut and the model body

A mathematical model accounts for the effect of the gap by treating interference and non-interference drags of the strut as additive terms. The extra drag (D_{ex}), equal to $D_m - D_s$, is the sum of the interference and non-interference drags:

$$D_{ex} = D_{I,rod} + D_{rod} + D_{I,sl} + D_{sl}\,, \tag{29}$$

where $D_{I,rod}$ is the interference drag from the rod, D_{rod} is the non-interference drag from the rod and the other two terms are analogous quantities for the sleeve.

The model treats the interference drags of the rod and sleeve as exponential functions of the gap width (Fig. 10). The interference drag from the rod increases from 0 as the widening gap exposes the rod, and approaches a maximum value ($D_{I,rod,max}$):

$$D_{I,rod} = D_{I,rod,max}(1 - e^{-G/\lambda})\,, \tag{30}$$

where e is the base of the natural logarithms (2.718), G is the width of the gap and λ is the space constant. $D_{I,rod}$ reaches 63.2 % of its maximum value when $G=\lambda$, and 95.0 % when $G=3\lambda$.

As the sleeve moves away from the body, the interference drag from the sleeve decreases from a maximum value ($D_{I,sl,max}$) and approaches zero:

$$D_{I,sl} = D_{I,sl,max}e^{-G/\lambda}. \tag{31}$$

D_{sl} decreases by 63.2 % from its maximum value when $G=\lambda$, and by 95.0 % when $G=3\lambda$.

The maximum interference drags of the rod and sleeve depend on the same interference length (h_I) for both, but different thicknesses (t_{rod} and t_{sl}) and drag coefficients ($C_{D,rod}$ and $C_{D,sl}$). For the rod,

$$D_{I,rod,max} = qt_{rod}h_IC_{D,rod}, \tag{32}$$

and for the sleeve,

$$D_{I,sl,max} = qt_{sl}h_IC_{D,sl}. \tag{33}$$

The non-interference drags of the rod and the sleeve depend on the strut length (h) and the width of the gap. For the rod,

$$D_{rod} = qt_{rod}GC_{D,rod}, \tag{34}$$

and for the sleeve,

$$D_{sl} = qt_{sl}(h-G)C_{D,sl}. \tag{35}$$

A space constant of 5 mm fits the data reasonably well (Fig. 7) when

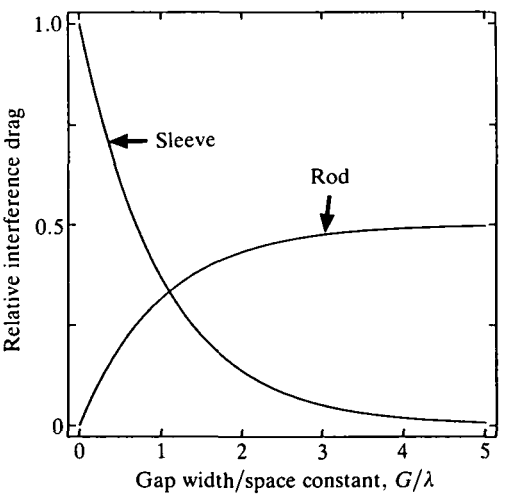

Fig. 10. Exponential relationships between interference drags of the rod and sleeve as the gap between the model body and the sleeve widens. The horizontal axis shows the gap width expressed as a proportion of the space constant. The vertical axis shows relative interference drag expressed as a proportion of the maximum interference drag from the sleeve.

$C_{D,rod}=C_{D,sl}=0.9$. The model indicates that 95 % of the interference drag arises from a region of the strut 15 mm long (3λ) nearest the body.

Hoerner (1965, pp. 8–10), using a different method, estimated that interference drag arises from a length of the strut that is 16 % of the maximum diameter of the object mounted on the strut. (The objects were bodies of revolution.) Applying this percentage to the effective diameter of the model falcon body (92.3 mm, equation 15) yields a strut length of 14.8 mm – essentially the same as the value estimated from the space constant.

List of symbols

C_D	drag coefficient of strut
$C_{D,B}$	drag coefficient of body
$C_{D,rod}$	drag coefficient of rod of special circular strut
$C_{D,sl}$	drag coefficient of sleeve of special circular strut
c	chord of strut
D_B	body drag
D_{ex}	extra drag (D_s+D_I)
D_I	interference drag
$D_{I,ex}$	extra interference drag ($D_{m,cal,sp}-D_{m,cal,sm}$)
$D_{I,rod}$	interference drag from rod of special circular strut
$D_{I,rod,max}$	maximum value of $D_{I,rod}$
$D_{I,sl}$	interference drag from sleeve of special circular strut
$D_{I,sl,max}$	maximum value of $D_{I,sl}$
$D_{I,0}$	interference drag for a strut with drag $D_{s,0}$ and measured drag $D_{m,0}$
D_m	measured drag of a body on a strut
$D_{m,cal,sm}$	measured drag of a body on a smooth calibration strut
$D_{m,cal,sp}$	measured drag of a body on a spoiled calibration strut
$D_{m,0}$	measured drag of a body on a particular strut
D_{rod}	drag of rod of special circular strut
D_s	strut drag
$D_{s,cal}$	drag of calibration strut
$D_{s,std}$	drag of standard strut
$D_{s,0}$	drag of a particular strut
D_{sl}	drag of sleeve of special circular strut
d_B	diameter of circle of area S_B
e	base of natural logarithms
f	fineness (c/t)
G	width of gap between sleeve of special circular strut and body
h	strut length
h_I	interference length
$h_{I,ex}$	extra interference length
q	dynamic pressure ($0.5\rho V^2$)

m	mass of intact bird
Re	Reynolds number
r	strut drag per unit length of strut
S_B	maximum cross-sectional area of body
t	strut thickness
t_{rod}	thickness of rod of special circular strut
t_{sl}	thickness of sleeve of special circular strut
V	air speed
w	corner dimension for simplified navy strut
λ	space constant for interference drag
μ	viscosity of air
π	ratio of circumference to diameter of a circle
ρ	density of air

This study was partly supported by a grant (453–5969) from the Duke University Research Council, and by a Cooperative Agreement (14–16–0009–87–991) between Mark Fuller, US Fish and Wildlife Service and Duke University.

References

BEISEL, R. B. AND DIEHL, W. S. (1923). Characteristics of streamline strut sections. *Bureau of Aeronautics, Tech. Note no.* **117**. Washington: Navy Department.

DIEHL, W. S. (1928). *Engineering Aerodynamics*. New York: The Ronald Press Co.

GOLDSTEIN, S. (1965). *Modern Developments in Fluid Mechanics*, vol. II. New York: Dover Publ.

GORLIN, S. M. AND SLEZINGER, I. I. (1966). *Wind Tunnels and Their Instrumentation*. Jerusalem, Israel: Israel Program for Scientific Translations.

HOERNER, S. F. (1965). *Fluid-Dynamic Drag*. Brick Town, NJ: S. F. Hoerner.

KU, H. H. (1969). *Precision Measurement and Calibration*. National Bureau of Standards Special Publ. **300**, vol. 1. Washington: US Govt Printing Office.

PANKHURST, R. C. AND HOLDER, D. W. (1952). *Wind-Tunnel Technique*. London: Sir Isaac Putnam and Sons, Ltd.

PENNYCUICK, C. J. (1989). *Bird Flight Performance*. Oxford: Oxford University Press.

PENNYCUICK, C. J., OBRECHT, H. H., III AND FULLER, M. R. (1988). Empirical estimates of body drag of large waterfowl and raptors. *J. exp. Biol.* **135**, 253–264.

POPE, A. AND HARPER, J. J. (1966). *Low-speed Wind Tunnel Testing*. New York: Wiley and Sons.

TUCKER, V. A. (1990). Body drag, feather drag and interference drag of the mounting strut in a peregrine falcon, *Falco peregrinus*. *J. exp. Biol.* **149**, 449–468.

TUCKER, V. A. AND HEINE, C. (1990). Aerodynamics of gliding flight in a Harris' hawk, *Parabuteo unicinctus*. *J. exp. Biol.* **149**, 469–489.

TUCKER, V. A. AND PARROTT, G. C. (1970). Aerodynamics of gliding flight in a falcon and other birds. *J. exp. Biol.* **52**, 345–367.

VOGEL, S. (1981). *Life in Moving Fluids*. Princeton: Princeton University Press.

VON MISES, R. (1959). *Theory of Flight*. New York: Dover Publ.